Supporting Information

Dmitrieva and Burg 10.1073/pnas.1404809111

SI Materials and Methods

Cell Culture. Primary human umbilical vein endothelial cells (HUVECs) (PCS-100–010; ATCC) were grown in Vascular Cell Basal Medium (PCS-100–030; ATCC) supplemented with Endothelial Cell Growth Kit-BBE (PCS-100–040; ATCC) and antibiotics (PCS-999–002; ATCC). Osmolality of this medium (control medium) was 270 mosmol/kg. High-NaCl medium was prepared by adding NaCl to the total osmolality of 290–380 mosmol/kg. All experiments were performed on logarithmically growing cells at about 80% confluence. To elevate NaCl, control medium was replaced by the high-NaCl medium. For proliferation curves shown on Fig. 1*A*, cells were counted at every passage. For all experiments, except those measuring long-term proliferation, cells were used at passages P1–P4.

Quantification of vWF secretion by HUVECs. vWF was measured in HUVEC supernatants using the von Willebrand factor (vWF) Human ELISA Kit (Ab108918; Abcam). Cells grown on 10-cm dishes were exposed to high NaCl. To maintain logarithmic growth, cells were reseeded to six-well plates 2 d after NaCl was increased and maintained in high NaCl for 2 d more. Some cells were returned to control medium for 2 d after 4 d in high NaCl. vWF secretion was measured during the last 20 h of exposure to high Na by replacing the media with fresh ones during that time. Then, the medium was collected, centrifuged at 3,000 × *g* for 10 min, and vWF concentration was measured in the supernatants. Cells were lysed and total protein measured as described below for Western blots. The amount of vWF secreted in 20 h was calculated from the collected volume of culture medium and concentration of vWF, normalized by total cell protein. The rate of secretion of vWF, when NaCl was elevated, was normalized by the rate in control medium.

Extraction of Protein from HUVECs and Western Blot. Cells were rinsed with PBS, adjusted with NaCl to the same osmolality as the medium, then lysed with RIPA buffer [50 mM Tris·HCl, 1% Nonidet P-40, 150mM NaCl, 1mM EDTA, 1 mM NaF, 1 mM Na3VO4, and protease inhibitors (Roche Diagnostics)]; 3× Laemmli sample buffer (Cell Signaling) was added to the lysates and samples were boiled for 5 min. Sample loading onto gels was equalized according to the total protein concentration measured before addition of Laemmli buffer. Primary antibodies were against vWF (A0082; Dako), NFAT5 (sc-13035; Santa Cruz Biotechnology), α-tubulin (691251; MP Biomedicals), and aldose reductase (kindly provided by Peter Kador, University of Nebraska Medical Center, Omaha, NE). Secondary antibodies were labeled with Alexa Fluor 680 nm dye (Invitrogen). Immunoblots were scanned and integral fluorescence (IF) from each band was measured using Odyssey Infrared Imaging System (Li-COR Biosciences).

Immunofluorescent Detection of vWF in HUVEC Cells. Cells grown on eight-chamber slides were fixed for 10 min in 2% (vol/vol) formaldehyde (18814; Polysciences, Inc.) at room temperature, washed with PBS, permeabilized with 0.1% Triton X-100 in PBS, and blocked with 3% (wt/vol) BSA for 1 h at room temperature. Slides were incubated with primary antibodies for vWF (A0082; Dako) at 4 °C overnight, followed by secondary antibodies labeled with Alexa Fluor 488 nm (green emission) (4412; Cell Signaling) at room temperature for 1 h. After two washes with PBS, cells were stained with 2.5 μg/mL DAPI (DNA stain) (D1306; Invitrogen) and mounted with ProLong Gold antifade reagent (P36930;Invitrogen). Pictures were taken by confocal microscopy using a Zeiss LSM 510 microscope (Carl Zeiss MicroImaging) with a 63× N.A. 1.4 oil-immersion objective.

RNA Extraction from HUVEC Cells and Quantification by Real-Time PCR. Cells were exposed to high NaCl for 4 d before measurement. Some cells were then returned to control medium for 2 d. Total RNA was extracted with RNeasy Mini Kit (74104; Qiagen). The RNA (1 μg) was converted to cDNA by reverse transcription using TaqMan high-capacity cDNA RT kit (4374966; Applied Biosystems). vWF and NFAT5 mRNA levels were measured by real-time PCR using human TaqMan gene expression assays (4331182; Life Technologies) on a 7900HT Fast Real-Time PCR System (Applied Biosystems). Quantification was performed by the Comparative CT method; 18S ribosomal RNA was used as an endogenous control (4319413E; Applied Biosystems) and was amplified in the same tube with the target. The relative copy number $[2^{-(\mathrm{Ct(vWF)}-\mathrm{Ct\ (18S\ rRNA)})}]$ of a target was calculated for each sample and normalized to the copy number in the corresponding control sample (270 mosmol/kg). The experiment was repeated five times.

ChIP. ChIP was performed using the Enzymatic Chromatin IP Kit (9003; Cell Signaling Technology) as described (1). HUVECs grown on 15-cm dishes were cross-linked with 1% formaldehyde for 10 min. Chromatin was digested with MNase to generate mainly mononucleosomes with a minor fraction of dinucleosomes. For each sample, chromatin containing 7 μg of DNA was immunoprecipitated with 10 μg of anti-NFAT5 antibody (13035; Santa Cruz Biotechnology) or with anti-normal rabbit IgG (2729; Cell Signaling Technology). Protein and RNA in samples were enzymatically digested, and the DNA was further purified. The number of DNA fragments containing target sequences in input chromatin and in chromatin immunoprecipitated (IP) with anti-NFAT5 and IgG were quantified by real-time PCR with SYBR-Green PCR Kit (204054; Qiagen). Three target sequences were quantified, one containing the NFAT5 binding site and two nearby sites outside of the NFAT5 binding site (the following section gives the target sequences). Quantification was performed by comparative CT method. The relative copy number of each target sequence for each IP sample was calculated as $2^{-(\mathrm{Ct(IP\ DNA)}-\mathrm{Ct\ (Input\ DNA)})}$. The number of copies of each target sequence in an NFAT5 ChIP was normalized by the copy number in an IgG ChIP. The experiment was repeated three times. Data are presented relative to control (270 mosmol/kg).

Primer Design for NFAT5 ChIP. Three primer pairs specific for the three regions close to the transcription start site of the vWF gene were designed using the Primer-BLAST tool (www.ncbi.nlm.nih.gov/tools/primer-blast/). One of these regions contains the NFAT5 binding sequence (TGGAAATGTCC); the other two regions do not, and served as negative controls. The regions of the vWF gene that were tested by ChIP are shown in Fig. 2*D*. Sequences of the primers are as follows: (*i*) (−) control 1: forward primer (GATTCTGCCTCTGGTGCCAT), reverse primer (CACATACCTCGCACTCTGCT); (*ii*) NFAT5 binding site: forward primer (CAGGGTACCAGAAGTGGGTG), reverse primer (GGTGAAGGTGGGGAGTGATG); and (*iii*) (−) control 2: forward primer (CTGTGAAGGTTCTGCGGAGT), reverse primer (CCCCAACAGGAGATGGCATT). Specificity of the primers was verified by gel electrophoresis of the PCR products. Each produced a single band.

Mice. Mice were purchased at age 3 mo from Taconic (129S6, 129SVE; Taconic Farms, Inc.) and housed in the National Heart, Lung, and Blood Institute (NHLBI) animal facility. All mouse studies were done under approved NHLBI animal study protocols and mice were housed in a facility accredited by the Association for Assessment and Accreditation of Laboratory Animal Care.

Water Restriction (9 d). The experiment design is shown in Fig. 3*A*. All mice received gelled food containing 30% water [1.7 mL of deionized water + 4 g of balanced purified rodent diet (AIN-76A; Research Diets) + 57 mg of agar per 5.7 g of the food]. Food was provided in excess in individual cups so the mice ate what they wanted. The control group had free access to water. Water-restricted mice did not get any additional water. Five control and five water-restricted mice were tested. For urine collection, mice were housed in metabolic cages (Hatteras Instruments). Urine was collected in vials under mineral oil to prevent evaporation. Collection vials were replaced every 24 h and urine osmolality was measured with a Fiske Model 210 Freezing-Point Micro-Osmometer (Fiske Associates).

Mouse Blood Collection. Blood was collected from the tails of the mice. The mice were placed under a heat lamp for 3–5 min to warm them and dilate blood vessels. After warming, the mice were placed in a restraining device from which their tails protruded. A small nick was made in the tail with a sterile scalpel blade. Four drops of the blood were collected into a tube containing 20 μL of heparin sodium (1,000 U/mL). Pressure was applied to the nick for 15–30 s to stop the flow of blood. Tubes were centrifuged at 1,000 × *g* for 10 min. Plasma was transferred to new tubes then centrifuged for 10 more minutes at 10,000 × *g* to remove platelets. The platelet-free plasma was stored at −80 °C. Collection tubes were weighed before and after the blood collection and after the plasma was transferred to calculate how much the plasma was diluted by the heparin. This dilution factor was used to calculate the concentrations of plasma proteins, vWF, and D-dimer. To prepare serum, blood was collected in the same way, but without heparin. The blood was allowed to clot by leaving it undisturbed at room temperature for 30 min, then the clot was removed by centrifuging at 4 °C for 10 min at 1,800 × *g*.

Measurement of Total Protein, vWF, and D-Dimer in Mouse Plasma. Total protein concentration in mouse plasma was measured using BCA Protein Assay Kit (23227; Pierce). vWF and D-dimer in the plasma were measured by Western blot. Equal volumes of plasma were loaded on the gel. Before loading, 3× Laemmli sample buffer supplemented with DTT (7722; Cell Signaling) was added to the samples and the mixtures were boiled for 5 min. Immunoblots used primary antibodies against vWF (A0082; Dako) and D-dimer (bs-3514R; Bioss) and secondary antibodies labeled with Alexa Fluor 680 nm dye (Invitrogen). The immunoblots were scanned and integral fluorescence from each band was measured using Odyssey Infrared Imaging System (LI-COR Biosciences).

Measurement of Plasminogen Activator Inhibitor 1 in Plasma. Plasminogen activator inhibitor 1 (PAI-1) was measured using a bead-based sandwich Luminex immunoassay technique (2). PAI-1 agarose beads and assay reagents were purchased from EMD Millipore (MCVD1-77AK). The assay was performed according to the manufacturer's instructions and PAI-1 was measured on a Luminex 100 System.

Measurement of Serum Sodium, Potassium, Blood Urea Nitrogen, Glucose, and Osmolality. The chemical parameters were measured with a Vitros 250 Chemistry System (Ortho-Clinical Diagnostics). Serum osmolality was measured with a vapor pressure osmometer (Vapro 5520; Wescor, Inc.).

RNA Extraction from Mouse Tissues and Analysis by Real-Time PCR. Tissues were collected in Allprotect Tissue Reagent (76405; Qiagen) at the end of the experiments and stored at −20 °C. Total RNA was extracted using AllPrep DNA/RNA Mini Kit (80204; Qiagen). RNA from lung was extracted using RNeasy Fibrous Tissue Mini Kit (74704; Qiagen). cDNA conversion and quantification of vWF, NFAT5, and aldose reductase (AR) mRNA by real-time PCR was performed as described above for HUVEC cells. Mouse TaqMan Gene Expression Assays (4331182; Life Technologies) for NFAT5, vWF, and AR were used.

Immunohistochemical Staining of Paraffin-Embedded Mouse Tissue Sections. Mouse tissues were fixed for 48 h in 4% paraformaldehyde at 4 °C then embedded in paraffin. Sections were cut and mounted on silanized slides by American Histolabs. Sections were stained with antibodies against vWF (A0082; Dako), CD31 (DIA 310; Dianova), and fibrinogen (4440-8004; AbD Serotec), as previously described (3). Visualization was with diaminobenzidine (DAB) (D22187; Molecular Probes), which generates a brown-colored oxidation product upon reaction with the HRP-labeled secondary antibody. Development of the brown DAB color was monitored to prevent oversaturation that would prevent quantification. A Nikon E800 Widefield Microscope was used for photography.

Quantification of vWF Protein Expression on Mouse Tissue Sections. To quantify vWF protein expression on the DAB-stained sections (discussed above), we used the yellow-CMYK channel method described by Pham et al. (4). They demonstrated that images in the CMYK yellow channel correlate with the immunohistochemistry DAB stain intensity. We extracted the CMYK yellow channel from the images of liver tissue sections stained with DAB for vWF (brown color) and with hematoxylin for nuclei (blue) (Fig. 4*B*) and quantified average yellow intensity per pixel as a measure of vWF protein expression. We processed the images according to Pham et al. (4), implemented with a Python script. The source image (R, G, B) is transformed to the final image (R', G', B') as follows:

$$(R', G', B') = (Y, Y, 0)$$

where $Y = 255 * \frac{(1-B)}{255-K}$ and $K = 255 - \max(R, G, B)$.

This transformation computes the yellow channel of the image by the RGB-to-CMYK format conversion and then loads that channel value back into the standard RGB image format. The effect of this transformation is to extract the yellow channel of the image. Examples of original images and images in the yellow channel after processing are given on Fig. S3. The Python script that performs this transformation is available upon request. Images of liver sections from five control and five water-restricted mice were analyzed; 10–15 images were taken from each section and their average intensity was calculated.

Statistical Analysis. Comparisons were performed by the nonpaired Student *t* test. $P < 0.05$ was considered significant. All data with $n = 5$ were tested by the Kolmogorov–Smirnov method for normality. All except AR mRNA passed the test. For AR, statistical significance was ascertained by the nonparametric Mann–Whitney test. For $n < 5$ (measurements of NFAT5 and AR proteins in HUVEC cells) normal distribution was assumed and Student *t* test was used. vWF protein secretion, vWF mRNA, NFAT5 protein and mRNA, and AR protein levels in HUVEC cells were analyzed for linear dependence on the level of NaCl. All of the statistical analyses were done using GraphPad InStat Software.

SI Results

Analysis of Association Between Plasma Sodium and Blood Level of vWF in Humans. To test for possible relation of plasma sodium concentration with that of vWF in humans, we analyzed the correlation of plasma sodium and vWF using data from the Atherosclerosis Risk in Communities (ARIC) Study. The data were obtained from the NHLBI Biologic Specimen and Data Repository Information Coordinating Center. Therefore, the results of our analysis do not necessarily reflect the opinions or views of the ARIC Investigators. ARIC is a study of cardiovascular disease in a cohort of 15,792 persons sampled from four US communities in 1987–1989. At baseline, 45- to 64-y-old members of sampled households in Minneapolis, Minnesota (selected suburbs); Forsyth County, North Carolina; Washington County, Maryland; and Jackson, Mississippi were enrolled (5). We used the results of the baseline clinical examination of the participants during their first visit.

The data were analyzed using SAS (SAS Institute Inc.) and SigmaPlot (Systat Software) software. We conducted multivariable regression analysis to assay the relation between the concentrations of serum sodium and vWF (6). Complete data were available for 14,679 participants. Participants with missing data were removed from the analysis. The following variables from the ARIC Study were used: sodium (mmol/L), vWF (IU/dL), glucose (mmol/L), blood urea nitrogen (BUN, mg/dL), creatinine (mg/dL), albumin (g/dL), body mass index (BMI, kg/m^2), and age (years). Estimated glomerular filtration rate (eGFR) was calculated using the Modification of Diet in Renal Disease equation (7): $\text{eGFR} = 170 \times \text{Serum Creatinine}^{-0.999} \times \text{Age}^{-0.176} \times (0.762 \text{ if Female}) \times (1.118 \text{ if Black}) \times \text{BUN}^{-0.170} \times \text{Albumin}^{+0.318}$.

We chose the variables to include in the analysis based on their known ability to affect the level of vWF. Diabetes, age, and chronic kidney disease (CKD) are all associated with increased levels of vWF (8, 9). Therefore, we included age, eGFR, glucose, and BMI in the list of candidates for inclusion in multivariable model as covariates to plasma sodium. Table S2 and Fig. S5 show the basic statistics and the distribution histograms for the chosen variables. Some of them are skewed. Therefore, for initial assessment of zero-order correlations, we used Spearman's rank correlation coefficient, a nonparametric measure of statistical dependence between two variables (Table S3). The zero-order correlation analysis did not reveal any association between sodium and vWF. However, both vWF and Na^+ levels are significantly correlated with other variables. Therefore, we proceeded with multiple regression analysis. We included Na^+, glucose, and eGFR in the final multivariable model. The reasons for this selection are (6) as follows. First, age was eliminated because its distribution is very far from normal (Fig. S5), and age is significantly correlated with all variables included in model (Table S3). Information about age is still preserved in the model through those correlations. Second, BMI was eliminated to reduce redundancy based on its relatively high correlation with glucose, which is a more interesting variable for our study, because glucose contributes to plasma osmolality and directly affects endothelia. Third, eGFR was included because it significantly correlates with vWF level but not with Na^+ and has a weaker correlation with glucose than other variables. In summary, our model includes the least correlated variables satisfying the requirement of independence in multivariable analysis, but at the same time preserves information about other variables, such as age and BMI, through correlations with them. For the final multivariable analysis, we transformed the vWF variable to make its distribution normal (Fig. S5).

Table S4 summarizes the results of the regression: The overall regression is statistically significant for all of the variables, namely, plasma Na^+, glucose, and eGFR, contributing to the plasma level of vWF [$F(3, 14{,}675) = 210$, $P < 0.001$]. We next removed eGFR from the model to see whether Na^+ and glucose can predict vWF without eGFR. The two-variable regression still is statistically significant, with both Na^+ and glucose being significant predictors of vWF level [$F(2, 14{,}676) = 289$, $P < 0.001$] (Table S5). Because regression coefficients are positive, we conclude that an increase in plasma Na^+ and/or glucose is accompanied by increased vWF.

Analysis of Association Between Plasma Sodium and Stroke Risk in the ARIC Study. The 10-y stroke risk at first visit was retrospectively calculated for participants in the ARIC Study based on the study outcomes and included in ARIC datasets (10). We used this information to test whether there is an association between plasma sodium concentration and the predicted stroke risk. The data were available for 13,630 participants. Participants with missing data were removed from the analysis. We conducted a multivariable regression analysis similar to the one that we performed to assess association between sodium and vWF. The analysis demonstrates that each of the predictor variables (plasma sodium, glucose, and eGFR) has a significant independent zero-order correlation with 10-y stroke risk (Table S6). In the multivariable model, all of the variables significantly ($P < 0.001$) contribute to the predicted risk of stroke [$F(3, 13{,}626) = 866$, $P < 0.001$] (Table S6). We next performed the same analysis on the cohort of participants without diabetes and without CKD (eGFR >60 mL·min^{-1}·1.73 m^{-2}) who had normal weight (BMI = 18.5–25 kg/m^2). In this "healthy" cohort ($n = 3{,}345$), all of the variables significantly ($P < 0.001$) contribute to predicted risk of stroke (Table S7). Thus, plasma sodium concentration is positively associated with 10-y risk of stroke predicted based on outcomes of the ARIC Study.

1. Dmitrieva NI, Cui K, Kitchaev DA, Zhao K, Burg MB (2011) DNA double-strand breaks induced by high NaCl occur predominantly in gene deserts. *Proc Natl Acad Sci USA* 108(51):20796–20801.
2. Khan SS, Smith MS, Reda D, Suffredini AF, McCoy JP, Jr. (2004) Multiplex bead array assays for detection of soluble cytokines: Comparisons of sensitivity and quantitative values among kits from multiple manufacturers. *Cytometry B Clin Cytom* 61(1):35–39.
3. Dmitrieva NI, Burg MB (2007) High NaCl promotes cellular senescence. *Cell Cycle* 6(24): 3108–3113.
4. Pham N-A, et al. (2007) Quantitative image analysis of immunohistochemical stains using a CMYK color model. *Diagn Pathol* 2:8.
5. Williams OD (1989) The Atherosclerosis Risk in Communities (ARIC) Study: Design and objectives. The ARIC investigators. *Am J Epidemiol* 129(4):687–702.
6. Royston P, Sauerbrei W (2008) Selection of variables. *Multivariable Model-Building: A Pragmatic Approach to Regression Analysis Based on Fractional Polynomials for Continuous Variables*, eds Royston P, Sauerbrei W (Wiley, New York), pp 23–52.
7. Levey AS, et al.; Modification of Diet in Renal Disease Study Group (1999) A more accurate method to estimate glomerular filtration rate from serum creatinine: A new prediction equation. *Ann Intern Med* 130(6):461–470.
8. Shen L, et al. (2012) Von Willebrand factor, ADAMTS13 activity, TNF-α and their relationships in patients with chronic kidney disease. *Exp Ther Med* 3(3):530–534.
9. Blann AD (2006) Plasma von Willebrand factor, thrombosis, and the endothelium: the first 30 years. *Thromb Haemost* 95(1):49–55.
10. Chambless LE, Heiss G, Shahar E, Earp MJ, Toole J (2004) Prediction of ischemic stroke risk in the Atherosclerosis Risk in Communities Study. *Am J Epidemiol* 160(3):259–269.

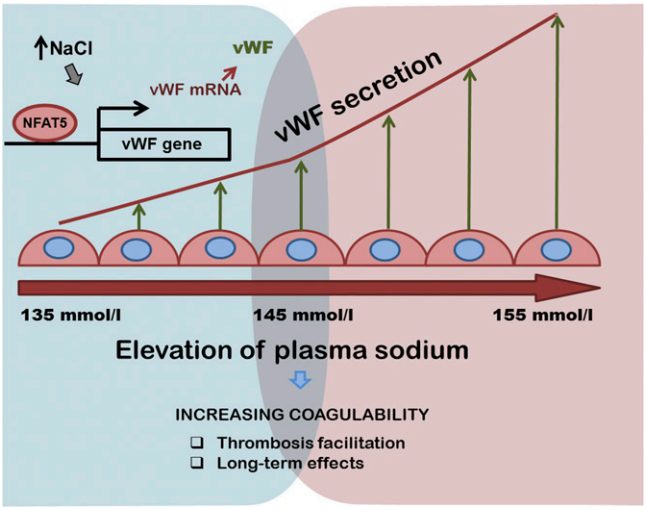

Fig. S1. Model summarizing the proposed relation between sodium, vWF, and thrombosis. Elevation of NaCl in extracellular fluid leads to graded increase of endothelial cell vWF mRNA, vWF protein, and of the rate of secretion of vWF from them. Increased vWF provides an explanation for the occurrence of thrombosis during hypernatremia. Even a small increase in plasma sodium (5 mmol/L), as the result of water restriction, increases vWF secretion from endothelial cells enough to increase blood vWF and stimulate thrombogenesis. Our findings suggest that hypernatremia-induced vWF secretion caused by insufficient water or excessive salt intake adversely affects cardiovascular health by increasing coagulability of blood and thus facilitating thrombotic events.

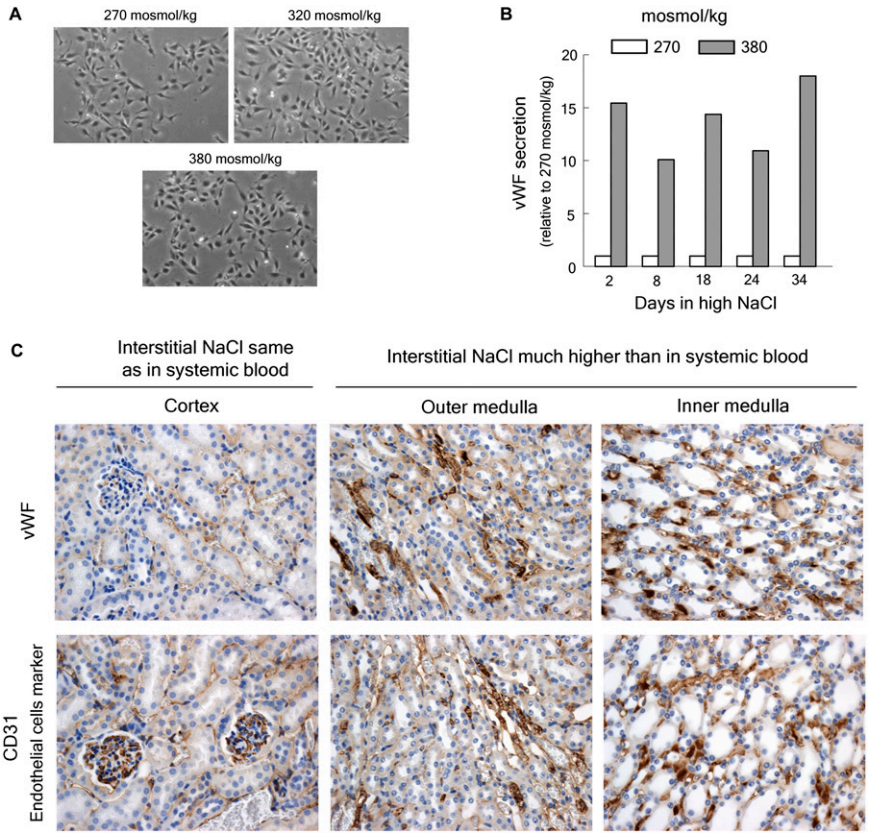

Fig. S2. High NaCl increases production and secretion of vWF from vascular endothelial cells. (*A*) Images of HUVEC cells grown in high-NaCl medium for 15 d. HUVEC cells adapt well to medium in which NaCl concentration is increased to total osmolality up to 380 mosmol/kg. (*B*) High NaCl increases vWF secretion rate from HUVEC cells and secretion stays elevated for many days as long as NaCl stays elevated. Primary HUVEC cells were exposed to media in which level of NaCl was elevated to total osmolality 380 mosmol/kg. The cells were exposed to such high-NaCl medium for 34 d. Cells were maintained in logarithmic growth by passaging them when they reached about 80% confluency. (*C*) Expression of vWF protein is higher in mouse renal medulla, where interstitial NaCl normally is high, than in cortex, where interstitial NaCl concentration is similar to that in systemic blood. Kidney tissue sections from normal mice show immunohistochemical localization of vWF in endothelial cells. Brown staining indicates vWF or CD31, a marker of endothelial cells; blue staining (hematoxylin) indicates nuclei. vWF is high in renal medullary endothelial cells but is almost entirely absent in the renal cortex.

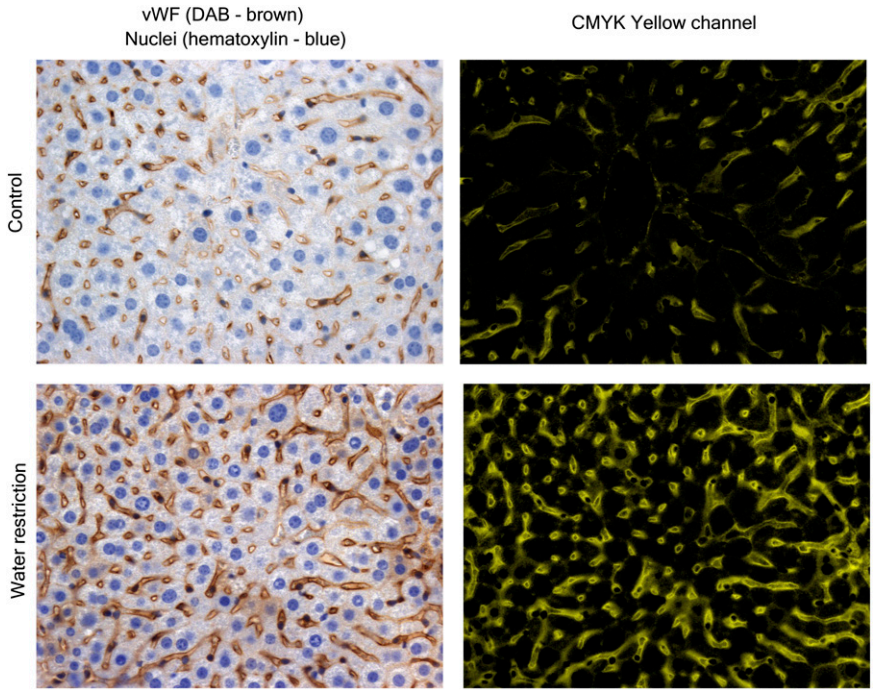

Fig. S3. Representative examples of CMYK yellow channel extraction from images of liver tissue sections stained for vWF using DAB chromogen and counterstained with hematoxylin. (*Left*) Original images. (*Right*) Images of extracted CMYK yellow channel. The pattern and intensity of the signal in the CMYK yellow channel (*Right*) corresponds in pattern and intensity to the brown DAB staining of vWF (*Left*). Also see *SI Materials and Methods* and Fig. 4 for full description of the vWF quantification.

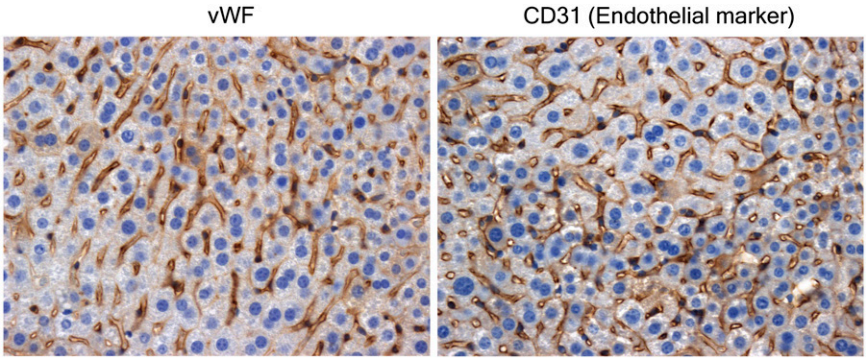

Fig. S4. Pattern of vWF staining correlates with the pattern of staining for the endothelial cell marker, CD31. Images of liver tissue sections stained for vWF and CD31, using DAB chromogen (brown) and counterstaining with hematoxylin (blue, nuclei).

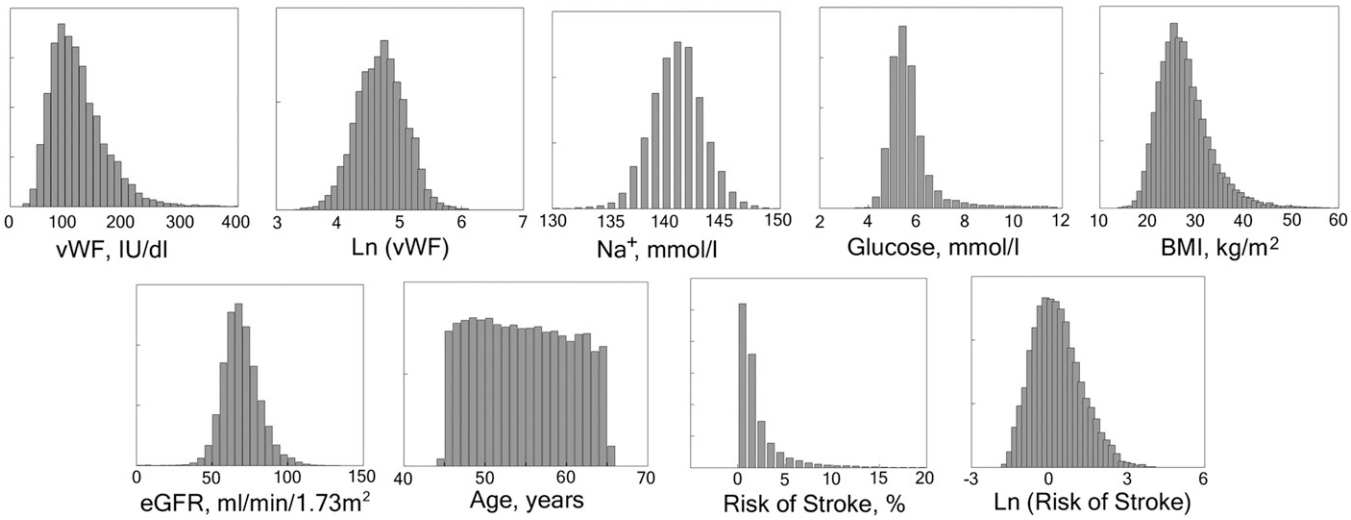

Fig. S5. Frequency distribution histograms for variables used in analysis of association of sodium with vWF and risk of stroke in the ARIC Study.

Table S1. Effect of water restriction on serum parameters of mice

Serum variable	Control	Water restriction
Sodium, mmol/L	145.1 ± 0.5	150.2 ± 1.3**
Osmolality, mosmol/L	294.4 ± 2.5	302.4 ± 3.6*
BUN, mg/dL	28.3 ± 1.6	37.3 ± 4.0*
Glucose, mg/dL	132.4 ± 3.3	136.2 ± 9.8
Potassium, mmol/L	5.9 ± 0.1	5.4 ± 0.1*

Mice were subjected to water restriction for 9 d. Blood was collected from tails and serum was prepared as described in *Materials and Methods*. *$P < 0.05$; **$P < 0.01$.

Table S2. Basic descriptive statistics for the variables used in analysis of the association between sodium and vWF in the ARIC Study

Variable	Mean	SD	5–95% percentiles
Na^+, mmol/L	141.0	2.4	137–145
vWF, IU/dL	118.7	48.6	58–206
BMI, kg/m^2	27.7	5.4	20.6–37.6
Glucose, mmol/L	6.1	2.3	4.7–9.6
eGFR, mL·min^{-1}·1.73 m^{-2}	69.1	12.4	51–90

Table S3. Spearman's rank correlation coefficients for the variables used in analysis of the association between sodium and vWF in the ARIC Study

Variable	vWF	Age	BMI	eGFR	Glucose
Na^+	0.00	0.06***	0.03*	0.00	−0.02*
vWF		0.19**	0.12**	−0.05***	0.14**
Age			0.00	−0.23**	0.14**
BMI				−0.02	0.32**
eGFR					0.01

*$P < 0.001$; **$P <$ 1.00E-06; ***$P <$ 1.00E-09.

Table S4. Multiple regression analysis of plasma level of vWF (transformed) with plasma Na^+, glucose, and eGFR as predictor variables (ARIC Study, $n = 14,679$)

Independent variable	Regression coefficient b_j	SE of b_j	t	P
Intercept	3.918	0.189	20.8	<0.001
Na^+, mmol/L	0.0050	0.0013	3.8	<0.001
Glucose, mmol/L	0.0344	0.0014	24.1	<0.001
eGFR, $mL \cdot min^{-1} \cdot 1.73\ m^{-2}$	−0.0018	0.0003	−7.2	<0.001

Na^+, glucose, and eGFR are significant predictors of vWF.

Table S5. Multiple regression analysis of plasma level of vWF (transformed) with plasma Na^+ and glucose as predictor variables (ARIC Study, $n = 14,679$)

Independent variable	Regression coefficient b_j	SE of b_j	t	P
Intercept	3.799	0.188	20.2	<0.001
Na^+, mmol/L	0.005	0.0013	3.7	<0.001
Glucose, mmol/L	0.0344	0.0014	24.1	<0.001

Na^+ and glucose are significant predictors of vWF. $F(2, 14,676) = 289$; $P < 0.001$.

Table S6. Multiple regression analysis of risk of stroke with plasma Na^+, glucose, and eGFR as predictor variables (ARIC Study, $n = 13,630$)

	Zero-order r (Spearman)			Multiple regression for ln(stroke risk)			
Variable	Stroke risk	Na^+	Glucose	Regression coefficient b_j	SE of b_j	t	P
Na^+	0.03*			0.028	0.0032	8.7	<0.001
Glucose	0.37**	−0.01		0.179	0.0035	50.7	<0.001
eGFR	0.07***	0.00	0.00	0.003	0.0006	4.8	<0.001

The analysis includes all ARIC Study participants ($n = 13,630$). Na^+, glucose, and eGFR are significant predictors of the risk of stroke. *$P < 0.001$; **$P <$ 1.00E-06; ***$P <$ 1.00E-09. Intercept, −4.872.

Table S7. Multiple regression analysis of risk of stroke with plasma Na^+, glucose, and eGFR as predictor variables (ARIC Study, $n = 3,345$)

Independent variable	Regression coefficient b_j	SE of b_j	t	P
Intercept	−5.491	0.879	−6.2	<0.001
Na^+, mmol/L	0.0153	0.0061	2.4	0.01
Glucose, mmol/L	0.396	0.031	12.8	<0.001
eGFR, $mL \cdot min^{-1} \cdot 1.73\ m^{-2}$	0.018	0.0015	11.8	<0.001

The analysis includes ARIC Study participants with no diabetes, BMI = 18.5–25 kg/m^2 and eGFR >60 $mL \cdot min^{-1} \cdot 1.73\ m^{-2}$. Na^+, glucose, and eGFR are significant predictors of the risk of stroke. $F(3, 3,341) = 105$; $P < 0.001$.